Molecular Collision Dynamics on Several Electronic States

T. J. Martínez*

Department of Chemistry, University of Illinois, Urbana, Illinois 61801

M. Ben-Nun†

Department of Chemistry and Biochemistry, University of California San Diego, La Jolla, California 92093-0339

R. D. Levine

The Fritz Haber Research Center for Molecular Dynamics, The Hebrew University, Jerusalem 91904, Israel

Received: March 5, 1997; In Final Form: May 6, 1997⊗

A time-dependent quantum mechanical method for propagating the wave function on several electronic states is discussed for the polyatomic case and illustrated by the quenching collision of a Na ($3p$ ^{2}P) atom by H_2. The specification of method is governed by the need to have a clear physical interpretation of the results, by the recognition that the motion on a given electronic state can often (but not always) be well approximated by classical mechanics, and by the need for a computational procedure that is simple enough to handle polyatomic systems. These desiderata are realized by the spawning technique which is discussed in detail. One more feature of the method is that it allows for a smooth interface with the methodologies of quantum chemistry so that the electronic structure problem can be solved simultaneously with the time propagation of the nuclear dynamics. The method is derived from a variational principle and so can yield quantum mechanically numerically converged results. The parameters that govern the numerical accuracy of the method are explicitly discussed with special reference to their physical significance. The quenching of a Na ($3p$ ^{2}P) atom by H_2 due to a conical intersection of two potential energy surfaces is used as a computational example since it illustrates many of the features of the method. This collision is found to be sticky and exhibits many sequential nonadiabatic couplings, each of which is localized in time, where the quenching probability per traversal of the conical intersection region is small. However, the accumulated transfer of population to the ground state can be significant since the duration of the overall transfer is spread over many vibrational periods of H_2.

I. Introduction

Collisions "of the second kind" involving the quenching of electronically excited atoms have been studied since the 1920s.[1−3] The seminal theoretical work of Landau and Zener[4−6] provided the notion of a localized "crossing region" where the probability of a nonadiabatic transition was high and thereby explained the often surprisingly large quenching cross sections. Stueckelberg[7] has added the refinement that since the "crossing" can occur either on the way in or on the way out, there will be a typical quantal interference phenomena. Teller[8−10] then made the key observation that the "no crossing" rule can fail in polyatomic systems and has analyzed the implications of passage near such a conical intersection of two potential energy surfaces.

For atom−atom collisions, stationary quantum mechanical scattering theory can be implemented (e.g., ref 11) and provides a validation of the ideas of Landau, Zener, and Stueckelberg. For polyatomic systems stationary quantum mechanical scattering methods can be discussed (e.g., refs 12 and 13 for atom−diatom collisions) but their computational implementation is by far more demanding. It is indeed only fairly recently[14] that the first full 3D stationary scattering computation has been reported, for the Na* + H_2 problem, the same system that we too use as an illustration. The development and applications of pump−probe experimental techniques has provided much impetus for the development of time-dependent quantum mechanical methods.[15] Such methods have proven suitable for treating the motion on more than one electronic state, and several recent versions have been proposed.[16−20] The method that we discuss below (see also refs 21 and 22) is fully quantum mechanical. However, in many ways it is best regarded as a descendent of classical methods. As a quantal method, it necessarily however does have elements of methodology similar to other quantal methods. For example, it uses a basis set but this basis is constructed and coupled in a special way as discussed in sections II and III.

Classical and semiclassical methods[4−6,23−29] have a clear, almost overwhelming, advantage in the number of degrees of freedom that can be handled. Strictly classical approaches are not permissible for nonadiabatic collisions because then the nuclei need to move under a single potential which implies the validity of the Born−Oppenheimer approximation—the very approximation whose breakdown is of interest. Perhaps the simplest way to allow for nonadiabatic transitions in a classical framework is the classical path approximation,[27,30,31] which allows the weights of the electronic states to change with time, while requiring that the nuclear dynamics be represented with a single trajectory. In this way, a single potential is operative, but this potential is a time-dependent weighted average of several electronic states. This scheme, while computationally very tractable and sometimes realistic, e.g., for describing fine structure transitions, has the limitation that in many problems of interest the motion of the nuclei in the different electronic states is qualitatively different, e.g., when a bound potential

† Present address: Department of Chemistry, University of Illinois, Urbana, IL 61801.

⊗ Abstract published in *Advance ACS Abstracts,* July 15, 1997.

S1089-5639(97)00842-6 CCC: $14.00

intersects a repulsive one. For these more common situations, one needs in one way or another to go beyond strict classical mechanics.

A classical method which has been often applied is the Tully surface hopping procedure.[24,32] The bare essence of that method is that a classical trajectory is propagated on a given electronic state, which means that the potential for the motion is well defined, until the trajectory reaches a localized region of effective nonadiabatic coupling. Then a decision is made whether to "hop" to a new electronic state or not. If a hop occurs, the trajectory is propagated on a new, again well-defined but different, potential—the potential appropriate to the new electronic state. The quantum mechanical methodology that we use has a similar philosophy, while the details are necessarily different. The variational nature of the methodology ensures that it can be carried to the level of numerical convergence, and this has been verified by comparison with numerical integration on a grid of the time dependent Schrödinger equation for one[21,22] (and two[33]) dimensional problems, including the three "standard" problems given by Tully.[32]

The method is not limited to such problems where the coupling of different electronic states is due to the breakdown of the Born−Oppenheimer separation. Applications have been reported[21,34−36] for the pump−probe technique where it is the external laser field that induces the coupling and also for a solvent-induced coupling between the bound and repulsive states of the I_2 molecule[35,36] where in the isolated molecule the two adiabatic states do not interact because of symmetry.

The principles guiding our procedure are discussed in section II, and the actual equations of motion with other technical details are given in section III. The method can be applied in either the adiabatic or diabatic electronic basis, and this and other aspects of the interface with quantum chemical computations of electronic structure are also discussed in section III. In section IV, we present computational results for electronic quenching in the collision of Na* and H_2.

II. Features of the Method

The essential ingredients in our method are as follows. We take the accumulated experience of three decades to imply that many essential dynamical features of the propagation of atoms on realistic potentials are well captured by classical mechanics. There are, of course, inherently quantal effects. The most obvious of these are interference[37−39] and tunneling. Additionally, there are more subtle dynamical effects (e.g., above barrier reflection) which are sometimes represented by adding a "quantum potential" to the classical equations of motion.[40] Notwithstanding the quantum features, classical mechanics does take care of much of the role of the potential. Hence the first operational conclusion: the computational procedure should have to deal only with corrections to the classical description and not with the classical description itself. In other words, the classical motion on a given electronic state should be, as much as possible, part of the zeroth-order description. For motion on a given electronic state, this implies that the "coupling" we need to deal with is due to corrections to the classical description. Below we refer to these as the "intrastate" coupling because such terms do not change the electronic state.

To obtain the true quantum mechanical converged wave function, it is necessary to retain the intrastate coupling terms which serve to correct the classical description of the motion on a given electronic state. We do so in the computations below. However, many quantal features average out when expectation values are computed.[39,41] Hence, for more averaged results it is often not unreasonable to partly or completely neglect these intrastate terms.

The other type of nonclassical terms in the equations of motion are those that represent the nonadiabatic coupling between different electronic states. These are the "interstate" coupling terms. We assume that typically these will be localized. The interstate couplings are handled by a procedure we term "spawning". This is our analogue of the "hopping" in "trajectory hopping", but the technical details are quite different. Spawning allows the wave function to bifurcate, with one part continuing on the initial electronic state while a second part evolves on a different electronic state.

As in the method of trajectory hopping, we spawn only when it is necessary, and the criterion for doing so is discussed below. Spawning is *not* instantaneous. The time evolution and the extent (and phase) of spawning are determined by the time-dependent Schrödinger equation. Because spawning is a dynamically dictated bifurcation of the wave function, it is a unitary time evolution. Probability, i.e., wave function normalization, is therefore inherently conserved.

Our method draws on the connection between the quantum mechanical time evolution of complex Gaussian functions and classical trajectories. This correspondence has a rich history, beginning with the recognition that the coherent states of a harmonic oscillator follow the classical equations of motion,[42,43] even when acted on by a force.[44] Heller championed the use of complex Gaussian functions as a numerical tool to study quantum dynamics on a single electronic state.[45] As summarized nicely in a review by Herman,[28] other workers have built on this framework, in the context of both single[46−64] and multiple[65−67] electronic state dynamics. Of all these methods, the one most closely related to our own is that of Sawada and Metiu[67] for one-dimensional wave functions. We have discussed the numerous differences when our method was tested,[21] of which perhaps the most prominent is our emphasis on connections with classical mechanics. Apart from numerical and interpretational advantages, these connections are what has enabled us to provide an efficient interface with quantum chemistry.[34,68−70]

The schematic outline of the method is as follows. A preliminary stage is to run classical trajectories for each electronic potential energy surface of interest. These are ordinary classical trajectories, without any regard for the other electronic states. The only sense in which the trajectories for the different electronic states are related is the trivial one that their total energy (electronic plus nuclear) needs to be about the same. (Not even exactly the same because the localized wave function is not an energy eigenstate.) In principle we need to include enough trajectories to representatively sample the energetically available phase space. In practice, far fewer are really needed; more on this below. In any case, with current computational capabilities this is readily manageable.

Each classical trajectory serves as a guide for the motion of the center of a nonspreading wave packet. The simplest such a packet is a frozen Gaussian.[45,71] These traveling wave packets, each of which carries, by construction, an electronic state label, are our time-dependent nuclear basis set. These wave packets are put aside in a store and not further used unless specifically called for by the spawning routine. Because these wave packets are waiting by the sidelines until they are called, it is not strictly necessary to generate them beforehand (and in practice we do not do so), but it helps to think of them in that way. ("*They also serve who only stand and wait*," Milton, Sonnet XV, 1652, except that our packets move and wait).

Next comes the quantum mechanical time propagation. In the most common case, when the collision starts on a given initial electronic state, initially only intrastate coupling is

operative. The wave function is then simple. It only has nuclear basis functions with a given electronic state label. Indeed, provided the nuclear basis functions and the desired initial state are of the same form, one nuclear basis function will often suffice. However, a more accurate procedure begins with a number of initial basis functions whose phase space centers are drawn from the Wigner distribution corresponding to the initial wave function.[72] This approach ensures that the basis functions which are required to do justice to the intrastate coupling are present in the later stages of the propagation.

All through the time propagation, the magnitude of the interstate, nonadiabatic coupling to the other states is monitored. When the nonadiabatic interstate coupling to a different electronic state exceeds a threshold value, we spawn new basis functions on this new state. The details of this spawning are discussed below, but the guiding principle is that the spawned functions should have maximal overlap with the "parent" basis function during the time when the coupling is maximal. In the impulsive limit, when the wave function spends very little time in the nonadiabatic coupling region, only a single spawned basis function is required. On the other hand, if the wave function lingers in the coupling region, it may be necessary to spawn more than one additional basis function for the new electronic state. The threshold value for designating coupling regions is one of the parameters that determines the numerical accuracy of the result. Strict convergence at the level of the wave function can require quite low values. Convergence at the level of observables, for example expectation values of position on a particular electronic state, can tolerate a higher threshold value.

After the spawning, the wave function has components on more than one electronic state. However, the computational effort is determined by how many nuclear basis states contribute to the wave function. At this point this number is still quite low. Once there is a component of the wave function on a new electronic state, it can spawn back into the initial electronic state and/or into other electronic states, etc. In practice we find that one can spawn very many times (as will be needed for $Na^* + H_2$[73]) before the implementation of the quantum time evolution becomes an issue.

To conclude, spawning allows the wave function to keep only those basis functions that have the greatest weight and therefore make the most important contribution to the nuclear dynamics. Because the nuclear basis states already, by construction, move along classical trajectories, the quantal time evolution only needs to handle the two nonclassical aspects, the interstate, nonadiabatic coupling, which is our prime interest, and the intrastate coupling, which corrects for the classical description on a given electronic state and which we retain so as to have a fully exact quantal method. In practice it should often be possible to take liberties with the latter type of coupling.

The criterion for spawning is the magnitude of the effective interstate coupling. In the diabatic representation, we define this as the magnitude of the coupling divided by the electronic energy gap evaluated at that point which is the center of the nuclear parent basis state. If this magnitude exceeds a preassigned threshold value, we launch a new nuclear basis state on the other electronic state. Two technical comments, concerning the later stages of time propagation, are in order here. After a while, when the two electronic states have been previously effectively coupled and one arrives at a point where a new spawn is called for, there may already be a nuclear basis state on the other electronic state surface localized just about where a need for a new basis state is indicated. In this case we do not spawn a new state because it will be nearly linearly dependent with an already existing state. Rather, we increase (or decrease) the weight of the existing state in the wave function. The extent and duration of this increment is determined by the equations of motion as derived from the Schrödinger equation in section III. The second point concerns the delocalization of the wave function. After a few spawns, the nuclear wave function on a given electronic state is a linear combination of a number of localized basis states. It is therefore no longer localized. In particular, (i) at similar times it can spawn new states onto a different electronic state at quite different locations and (ii) expectation values computed for such a wave function do not necessarily have small dispersions, e.g., the mean value of a coordinate is not necessarily a good indicator of the location of the wave function centroid.

III. Formalism

This section provides a quantitative and detailed description of the method for the general case of several nuclear degrees of freedom. (The computational example of section IV is nine-dimensional.) Technical aspects of a more specialized nature, such as the choice of time step and the associated checks for numerical convergence, are provided but are also discussed in more detail elsewhere.[33] We do however discuss why our method remains practical also in the multidimensional case and what steps are taken to make it as efficient as possible. Also discussed is the nature of the possible interface to quantum chemical codes which enables one to simultaneously determine the electronic structure and the nuclear dynamics. Explicit expressions are given for the gradients of the electronic wave functions which the method uses as an input when the electronic structure is determined "on the fly". These gradients are available as standard output in so-called quantum chemical gradient routines.[74−76] We present a multidimensional saddle-point approximation (cf. ref 69 for the one-dimensional case), which greatly facilitates the interface with electronic structure problems. Finally, it is emphasized that, with suitable changes in the nature of the couplings, the method is equally applicable in both the adiabatic and diabatic representations.

(A) The Total Wave Function. The total time-dependent wave function of the system is expanded as a weighted sum over electronic states of normalized wave functions. Each component in the sum is a product of an electronic and a (time dependent) nuclear wave function

$$\Psi = \sum_I C_I(t)\phi_I(\mathbf{r};\mathbf{R})\,\chi_I(\mathbf{R};t) \tag{3.1}$$

(Throughout this paper bold letters are used to denote vectors and matrices.) The wave functions of the electronic states are taken to be orthonormal over the electronic coordinates

$$\int \mathrm{d}\mathbf{r}\,\phi_{I'}^*(\mathbf{r};\mathbf{R})\,\phi_I(\mathbf{r};\mathbf{R}) = \delta_{I,I'} \tag{3.2}$$

and they are allowed to depend parametrically on the nuclear coordinates, **R**. If the electronic states are adiabatic, then this dependence is due to the usual electronic part of the total Hamiltonian being parametrized by the positions of nuclei. For a diabatic basis, the dependence on **R** will be much smoother[77] or altogether absent. The dynamical equations of motion as derived below assume that the matrix elements of the *total* Hamiltonian in the electronic basis are a given input. Below we shall discuss the question of generating this required input simultaneously with propagation of the wave function. If the electronic basis is adiabatic, then, by definition, it diagonalizes the electronic part of the Hamiltonian and so the only off-diagonal matrix elements of the total Hamiltonian in the electronic basis are due to the nuclear kinetic energy operator.

In contrast, the diabatic basis is chosen so that the latter is (exactly or effectively) diagonal, and it is the electronic Hamiltonian that has off-diagonal matrix elements.

The nuclear wave functions are normalized but need not be orthogonal to one another. The (complex) amplitudes C_I determine the population, $|C_I|^2$, and the degree of coherence of the different electronic states. To determine them, it is sufficient that the electronic wave functions of the different states are orthogonal. The initial conditions in the experiment specify the values of these amplitudes at early times, $t \rightarrow -\infty$. Typically, only one particular electronic state will be initially populated so that

$$|C_I|^2 \xrightarrow{t \rightarrow -\infty} \delta_{I,I'}$$

(B) The Nuclear Wave Functions. The time-dependent nuclear wave function for the *I*th electronic state is represented as a linear combination of (multidimensional) traveling basis wave functions, with time-dependent weights:

$$\chi_I(\mathbf{R};t) = \sum_j \mathrm{d}_{I,j}(t)\, \chi_j^I(\mathbf{R};\bar{\mathbf{R}}_j^I(t),\bar{\mathbf{P}}_j^I(t),\gamma_j^I(t),\alpha_j^I) \qquad (3.3)$$

where each time-dependent basis state is centered about a classical trajectory which is determined by the potential of the *I*th electronic state. This potential will be a diabatic or an adiabatic one according to which electronic basis set is being employed. In an ideal world, each component in the sum (3.3) would suffice to describe the quantum mechanical motion in the absence of coupling between different electronic states. The first approximation replaces this ideal by a practical approximation of a traveling Gaussian state, where this (multidimensional) Gaussian is most simply constructed as a product of (one-dimensional) Gaussian functions for each nuclear degree of freedom. Of course, we will need to correct for the Gaussian not being an exact solution for any but a harmonic potential, and this will give rise to the intrastate coupling terms which will be discussed below.

Explicitly, it is most convenient to use a Cartesian coordinate system and write each term in eq 3.3 as a product of $3N$ (one-dimensional) Gaussians:

$$\chi_j^I(\mathbf{R};\bar{\mathbf{R}}_j^I(t),\bar{\mathbf{P}}_j^I(t),\gamma_j^I(t),\alpha_j^I) = \exp(i\gamma_j^I(t))\prod_{\rho=1}^{3N}\chi_{\rho j}^I(R_\rho;\bar{R}_{\rho j}^I(t),\bar{P}_{\rho j}^I(t),\alpha_{\rho j}^I)$$

$$\chi_{\rho j}^I(R_\rho;\bar{R}_{\rho j}^I(t),\bar{P}_{\rho j}^I(t),\alpha_{\rho j}^I) \equiv (2\alpha_{\rho j}^I/\pi)^{1/4}\exp(-\alpha_{\rho j}^I(R_\rho - \bar{R}_{\rho j}^I)^2 + i\bar{P}_{\rho j}^I(R_\rho - \bar{R}_{\rho j}^I)) \qquad (3.4)$$

Here, ρ, $\rho = 1, ..., 3N$ enumerates the N atoms in the system and their three Cartesian coordinates, and the time-dependent parameters are determined so that each Gaussian state is centered along a classical trajectory:

$$\partial\bar{R}_{\rho j}^I(t)/\partial t = \bar{P}_{\rho j}^I(t)/M_\rho$$

$$\partial\bar{P}_{\rho j}^I(t)/\partial t = (\partial V_{I,I}(R)/\partial R)\bar{R}_{\rho j}^I(t)$$

$$\partial\gamma j^I(t)/\partial t = -VI,I(\bar{\mathbf{R}}j^I(t)) + \sum_\rho^{3N}((\bar{P}_{\rho j}^I(t))^2 - 2\alpha_{\rho j}^I)/2M\rho \qquad (3.5)$$

In eq 3.5 M_ρ is the mass of the ρth atom (in order not to make the notation too complicated, we use the index ρ to denote the mass of an atom although in principle it denotes a Cartesian coordinate of a particular atom) and each Gaussian has a time-independent width, $\alpha_{\rho j}^I$. In the special case of harmonic potentials, the natural choice for this width is related to mass and frequency.[78,45] However, for general potentials, the choice is not clear, and the width is best viewed as an arbitrary parameter characterizing the basis set. In the cases we have examined to date, the results (e.g., branching ratios) are rather insensitive to the particular value chosen. Note that a single nuclear phase, $\bar{\gamma}_j^I(t)$, propagated using the Lagrangian, is associated with each multidimensional Gaussian (cf. eq 3.4). The nuclear phase will govern the Stueckelberg type interference between different nonadiabatic transitions.

Equation 3.5 consists of a set of $(6N + 1)n$ coupled first-order ordinary linear differential equations, where n is the number of spawned basis functions. A single classical trajectory on a given electronic state requires solving $6N + 1$ such equations (the extra 1 is due to the nuclear phase γ). The computational effort required to solve (3.5) is n times greater than that required for a single classical trajectory. The additional computational effort is due to the two main points of the method: the dynamics occurs on I coupled electronic states and the spawning which serves to keep the basis size as small as possible. Other practical aspects of the propagation scheme are discussed in subsection F below.

The coefficients $d_{I,j}$ in eq 3.3 are time dependent, and their equation of motion is discussed in subsection C. Their initial values are determined by the initial state before the collision. When we speak of "a single run", we mean a computation where only one particular nuclear basis state is initially populated. Note that this need not be a typical initial state because it is not a stationary state of the Hamiltonian for the noninteracting partners. (It is a coherent-like state.) A stationary state needs to be represented as a linear combination of several nuclear basis states. A single run generates however a bona fide wave function. One of our observations in the results section is that single runs provide much more dynamical detail than stationary initial states, where for the latter some detail is washed out by the averaging inherent in representing the stationary state as a linear combination of basis states. The experimental realization of this observation is of course pump−probe time-domain spectroscopy as practiced by Zewail and others.[79,80]

The use of Gaussian-shaped wave functions for individual degrees of freedom has the clear advantage that it is easy to center the wave function along a classical trajectory. However, the Gaussian basis states are not orthogonal and tend to become, with time, overly linearly dependent which requires care as is discussed below. Also, in practice one wants to use as few basis states as possible, which means that the intrastate coupling terms should be as small as possible. Thus, other choices are worth exploring.

(C) The Equations of Motion. The time dependence of the total wave function requires solving for the time evolution of the coefficients $D_j^I \equiv C_I d_{I,j}$, which are the quantal amplitudes for being in the nuclear basis state j on the electronic state I at time t. The number of these coefficients is determined by how many electronic states are included (i.e., by the range of the index I) and by how many nuclear basis states are required (i.e., by the range of the index j) but is *not* directly influenced by the number of nuclear degrees of freedom, i.e., the number of atoms. Using a Gaussian basis set (or any other nonorthogonal basis) for the nuclear wave function (Eqs 3.3 and 3.4) a set of coupled equations of motion for the coefficients is obtained by taking the scalar product of the time-dependent Schrödinger equation for the total wave function on each nuclear basis state.

This prescription ("Dirac's variation of constants") is variational in nature and will converge given enough basis states. However, the time propagation is unitary regardless of the basis size and so there is no obvious "flag" for failure to converge. This point is further discussed in subsection F and in ref 33.

The resulting equation of motion is

$$\frac{\mathrm{d}D_j^I}{\mathrm{d}t} = \frac{\mathrm{d}(C_I \mathrm{d}_{I,j})}{\mathrm{d}t} = -i\sum_{k,l}(\mathbf{S}_{I,I}^{-1})_{j,k}\{(\mathbf{H}_{I,I} - i\dot{\mathbf{S}}_{I,I})_{k,l}D_l^I + \sum_{I\neq I'}(\mathbf{H}_{I,I'})_{k,l}D_l^{I'}\} \quad (3.6)$$

The equation is written so as to distinguish the intra ($I = I'$) and inter ($I \neq I'$) state coupling terms. The matrices **H** and **S** are defined by integration over the electronic coordinates only, e.g.

$$\hat{H}_{I,I'} \equiv \int \mathrm{d}\mathbf{r}\, \phi_I^*(\mathbf{r};\mathbf{R})\, \hat{H}\phi_{I'}(\mathbf{r};\mathbf{R}) \quad (3.7)$$

The orthonormality eq 3.2, of the electronic states means that **S** acts as the identity matrix but **H** is an operator on the nuclear coordinates. Equation 3.6 requires as input the matrix elements of the **H** and **S** matrices over the nuclear basis states. First note that **S** is not diagonal in the nuclear indices because it is the (time-dependent) overlap matrix of different Gaussians which are not orthogonal to one another:

$$(\mathbf{S}_{I,I})_{j,k} \equiv \langle \chi_j^I | \chi_k^I \rangle \quad (3.8)$$

The intrastate ($I = I'$) coupling in the equation of motion is due both to the Hamiltonian matrix elements:

$$(\mathbf{H}_{I,I})_{j,k} \equiv \langle \chi_j^I | \hat{H}_{I,I} | \chi_k^I \rangle \quad (3.9)$$

and to the time dependence of the overlap:

$$(\dot{\mathbf{S}}_{I,I})_{j,k} \equiv \langle \chi_j^I | \partial\chi_k^I/\partial t \rangle \quad (3.10)$$

The interstate coupling ($I \neq I'$) is similar to (3.9) except that it is defined by the elements of the Hamiltonian which are off-diagonal in the electronic state index:

$$(\mathbf{H}_{I,I'})_{j,k} \equiv \langle \chi_j^I | \hat{H}_{I,I'} | \chi_k^{I'} \rangle$$

In the interstate coupling there is no overlap term because **S** is diagonal in the electronic state index. Below, in subsection D, we further discuss the coupling terms 3.9 and 3.11.

The equations of motion (3.6) are the "full multiple spawning" method (FMS) which generates not only expectation values but also a wave function that provides a reliable approximation, in fact as close as desired, to the numerically exact quantum dynamics. The only numerical problem is the need to avoid excessive linear dependence of the Gaussian basis functions,[60] and this can be handled using a regularization of the overlap matrix via singular value decomposition.[81] For problems of one[22] or two[33] nuclear degrees of freedom, when exact quantal propagation[15] can be readily implemented, there is already a savings in computational effort using FMS (in our experience this is often around a factor of 5−10, depending on the details of the problem). More importantly, the FMS remains a viable method for larger systems, while numerically exact quantal (grid-based) propagation[15] is not feasible for more than six dimensions given current computational facilities. We demonstrate this advantage by examining a problem with nine degrees of freedom in section IV. The FMS equations of motion allow for quantal interference between nuclear wave packets on the various electronic states. The importance of this will be evident in the computational example below.

(D) Inter- and Intrastate Coupling. In the multidimensional case, there are three points that need to be explicitly addressed regarding the matrix elements of the total Hamiltonian which are needed as an input for the equations of motion 3.6. First is the question of the electronic basis set. The Born−Oppenheimer basis set diagonalizes the Hamiltonian for (every) fixed position of the nuclei. The resulting electronic wave functions will depend on the nuclear coordinates **R**, particularly so near a conical intersection or an avoided crossing. The matrix elements 3.9 and 3.11 are then due to the nuclear kinetic energy operator

$$(\mathbf{H}_{I,I'})_{j,k} = \langle \chi_j^I | \hat{H}_{I,I'} | \chi_k^{I'} \rangle = \langle \chi_j^I | E_{I,I'}(\mathbf{R}) | \chi_k^{I'} \rangle \delta_{I,I'} + \langle \chi_j^I | \hat{T}_{I,I'} | \chi_k^{I'} \rangle$$
$$\hat{T}_{I,I'} = \hat{T}\delta_{I,I'} + 2A_{I,I'}\nabla + B_{I,I'} \quad (3.12)$$

where $E_{I,I'}(R)$ is the potential energy surface for the Ith electronic surface and $\hat{T}$ is the usual nuclear kinetic energy operator, which is particularly simple in the Cartesian system of coordinates that we use. The non-Born−Oppenheimer terms, explicitly given by

$$\hat{T} = -\sum_{\rho=1}^{3N}(\hbar^2/M_\rho)\nabla_\rho^2$$

$$\hat{A}_{I,I'} = -\sum_{\rho=1}^{3N}(\hbar^2/M_\rho)\int \mathrm{d}\mathbf{r}\, \phi_I^*(\mathbf{r};\mathbf{R})\nabla_\rho \phi_{I'}(\mathbf{r};\mathbf{R})$$

$$\hat{B}_{I,I'} = -\sum_{\rho=1}^{3N}(\hbar^2/M_\rho)\int \mathrm{d}\mathbf{r}\, \phi_I^*(\mathbf{r};\mathbf{R})\nabla_\rho^2 \phi_{I'}(\mathbf{r};\mathbf{R}) \quad (3.13)$$

are the interstate terms that couple the different electronic states.

It is also possible to choose a diabatic basis which in practice means that the **R** dependence is either weak or even nonexistent so that the nuclear kinetic energy operator has no off-diagonal matrix elements between electronic states. On the other hand the electronic energy is not diagonal so that (3.12) is replaced by

$$(\mathbf{H}_{I,I'})_{j,k} = \langle \chi_j^I | \hat{H}_{I,I'} | \chi_k^{I'} \rangle = \langle \chi_j^I | E_{I,I'}(R) | \chi_k^{I'} \rangle + \langle \chi_j^I | \hat{T} | \chi_k^{I'} \rangle \delta_{I,I'} \quad (3.14)$$

with $E_{I,I'}(R)$, $I \neq I'$ being the potential coupling between different diabatic states.

While either the diabatic or adiabatic representation can be used, an important consideration is that the effective interstate coupling terms be localized. This will almost invariably favor the Born−Oppenheimer, adiabatic basis. The reason for preferring a localized coupling region is that this brings one closer to the impulsive coupling limit wherein fewer basis functions need to be spawned on the other electronic state. Furthermore, localized coupling makes a stronger case for evaluation of the multidimensional integrations required in (3.12) or (3.14) using saddle-point approximations as discussed below. When a conical intersection is involved, however, the adiabatic interstate coupling is singular and discontinuous at the intersection point. To avoid the resulting numerical instability, we use the diabatic representation in the example presented below.

The third point about the coupling is that it is often useful to approximate the integration over the nuclear coordinates by a saddle-point procedure. This is different than a Condon-like approximation because the motivation is as much the localized

nature of the coupling as the localized nature of the overlap. The operational procedure is given by a first-order saddle-point approximation to the matrix element of a function in position space ($f(\mathbf{R})$)

$$\langle \chi_j^I | f(\mathbf{R}) | \chi_k^{I'} \rangle \cong \langle \chi_j^I | \chi_k^{I'} \rangle f(\bar{\mathbf{R}}) \tag{3.15}$$

where $\bar{\mathbf{R}}$ is the location of the centroid of the product of the two basis functions j and k. Second- and higher-order approximations[69] are also possible, but they require derivatives of the interstate coupling which may not always be available (e.g., when quantum chemistry is used to generate the potential energy surfaces and their couplings).

(E) Interface with Quantum Chemistry. The methods of quantum chemistry determine electronic wave functions and their eigenvalues by diagonalizing the Hamiltonian for a fixed position of the nuclei. By repeating this procedure at different configurations of the nuclei, one can map the entire potential energy surface(s). In the multidimensional case, fitting an analytical function to the numerical points is, at best, not easy. It would be much better to use the raw output. But the raw output is local in **R**. This would be fine for classical mechanics because "analytical derivative" methods[74−76] provide not only the eigenvalues and eigenfunctions but also their gradients. The classical equations of motion are essentially local in that all that is needed are the forces (i.e., the gradients of the potential, cf. (3.5)). But the quantum dynamics of the nuclei is not local. The saddle-point approximation (eq 3.15) offers the simplest resolution of this dilemma.

The approximation (3.15) means that one can solve the electronic structure problem "on the fly", that is, simultaneously with the propagation of the nuclear dynamics. As one reaches a new configuration of the nuclei, quantum chemistry is asked to determine the gradients which are used (i) to propagate the guiding trajectory to a new position, using eq 3.5, (ii) to evaluate the intrastate coupling terms using eq 3.15, and (iii) to evaluate the interstate, nonadiabatic terms ($A_{I,I'}$ and $B_{I,I'}$) in eqs 3.12−3.13 and then use eq 3.15 for their nuclear matrix elements. In our experience, the second-derivative term, $B_{I,I'}$, is often much smaller and, as a first approximation can be neglected. Now one can take the next time step, and begin again. See also ref 69 on how to most efficiently take the time step.

The interface with quantum chemistry has, so far, only been reported for the one-dimensional case (i.e., for diatomics or for atom−atom collisions).[34,68] Work is however in progress on much more elaborate applications.[70] We also note that although the interface with quantum chemistry has so far used ab initio methods, there is nothing to prevent the use of cruder semiempirical methods. Indeed, when ab initio methods are used, the solution of the electronic problem forms the bulk of the effort, and it is thus natural to consider the possibility of using the computationally more tractable semiempirical methods.

(F) Spawning. In the multidimensional case, the technique of spawning is essential for keeping the basis size manageable. First note that, necessarily, the equation of motion is solved by propagating in finite time steps. On the other hand, in describing a collision the initial wave function is, usually, confined to a particular electronic state and possibly also to a particular nuclear basis function. After some time steps, due to nonadiabatic transitions (or possibly to an external laser pulse, see e.g., refs 22, 35, 36, and 82), the total wave function must develop a presence on other electronic states. This is brought about by the spawning procedure as follows. An effective nonadiabatic coupling is defined by

$$H_{IJ}^{eff}(\mathbf{R}) = \begin{Bmatrix} \left| \dfrac{\langle \phi_I(\mathbf{r};\mathbf{R}) | \hat{H} | \phi_J(\mathbf{r};\mathbf{R}) \rangle}{E_{I,I}(\mathbf{R}) - E_{J,J}(\mathbf{R})} \right| & \text{diabatic} \\ \left| \sum_\rho \left\langle \phi_I(\mathbf{r};\mathbf{R}) \left| \dfrac{\partial}{\partial \mathbf{R}_\rho} \right| \phi_J(\mathbf{r};\mathbf{R}) \right\rangle \mathbf{v}_\rho \right| & \text{adiabatic} \end{Bmatrix} \tag{3.16}$$

where $\mathbf{v}$ is the velocity vector. In the diabatic representation, the nonadiabatic coupling depends only on the nuclear coordinates, but in the adiabatic representation it depends on the nuclear velocity. In both cases, this "effective coupling" is introduced so that we will have a criteria for spawning which depends only on the occupied basis function. This allows us to avoid spawning attempts when they are not called for. A necessary condition for spawning is that the effective coupling reaches a threshold value (preassigned and determined by numerical convergence requirements). If the other electronic state is empty, then this is also a sufficient condition and a new nuclear basis state, on the so far unoccupied electronic state, is added to the total wave function. This new nuclear state is localized at the same position as the nuclear state on the already occupied electronic state. The new nuclear state is called from the "store" as discussed in section II. An efficient way to build such a store is to take advantage of the observation that the time axis is, de facto, discrete. Therefore, take the initially occupied nuclear basis state and propagate it on its own electronic state. At each discrete point in time and for each possible electronic state, specify a nuclear basis function which is of maximal overlap with the present functional form of the initially occupied nuclear basis state. These states are then available if they are needed and at that discrete time point when they are needed they will have a maximal overlap, by construction. If only one function is to be spawned per nonadiabatic event, one should propagate through the coupling region and choose the spawned function such that it is of maximal overlap with the initially occupied nuclear basis function at the time when the coupling is also maximal. This special way of preparing a basis set of nuclear states takes advantage of the detailed nature of the computation. It minimizes the number of nuclear basis states that are actually needed to be present in the full wave function at the price that the basis is "tailored" to the particular run. For multidimensional problems the savings in the occupied basis size is however an important consideration.

The full condition for spawning is the necessary condition that the effective coupling warrants a spawn and the sufficient condition that the other electronic state has no occupied nuclear basis state of high overlap with the nuclear state on the initial electronic state. After a while it is no longer obvious that the sufficient condition is automatically satisfied. Rather, it too needs to be checked. If it happens that there is an occupied nuclear basis state of high overlap with the nuclear state on the initial electronic state, then no spawning is allowed. Instead, the already finite amplitude of that nuclear state is allowed to change, and this is taken care of, automatically, by the equation of motion (3.6). The technical reason for imposing the sufficient condition is the near linear dependence of nuclear basis states which are too close to one another. This overcompleteness of the Gaussian basis speaks against spawning willy-nilly and is consistent with our general philosophy[22] that the nuclear basis set should "tile" the available phase space.[83−86]

(G) Numerical Considerations. It is worthwhile to explicitly state the numerical parameters which exist in the method. First of all, there is the time-independent width of the nuclear basis functions, α_ρ^I. This parameter is in principle arbitrary, because for any desired value, the set of all nuclear basis functions of

the form (3.4) is overcomplete. However, in practice basis set convergence might be achieved much faster for some choices than others. Although this issue deserves further consideration, we have not found that the resulting dynamics is overly sensitive to this parameter.

Second, there are the various thresholds which can be systematically varied to approach convergence. The first of these is the value of the effective coupling which triggers spawning. Given localized interstate coupling, it is not difficult to choose this threshold, and in general we find it easy to demonstrate convergence with respect to its variation. The recommended procedure is to run a few sample trajectories and examine the time dependence of the "effective coupling", choosing a threshold value which does not miss any of the resulting nonadiabatic events (indicated by "spikes" in the effective coupling).

A third numerical parameter is the criterion for determining if a basis function that is to be spawned is redundant with other basis functions on the relevant electronic state. We use the maximum overlap of the proposed function with all other basis functions on the same electronic state as a measure of this redundancy. If this value exceeds a threshold, the function is declared redundant and the spawn is aborted. Because we do not neglect the overlap of the nuclear basis functions in solving (3.6), convergence is approached as this parameter is taken closer to unity. Setting this to a value less than unity is simply a numerical convenience which avoids the wasteful spawning of functions which will in any case be removed when the overlap matrix is inverted.

Finally, there is the number of spawned functions per "event." We have mentioned above the two limiting cases—attempting to spawn every time step and spawning exactly once while in the coupling region. In general, the former limit is wasteful, and the latter may not be sufficient. A systematic approach to convergence is possible by introducing a third parameter which is the number of spawn attempts, N_s, per traversal of the coupling region. The time axis is divided into N_s intervals, and the spawned function is designed to have maximal overlap with its parent when the coupling is maximal in its designated time interval. Convergence is achieved when the time intervals are of comparable duration to the amount of time it takes the spawned function and its parent to separate in phase space. If the potentials for the coupled electronic states are very similar, convergence is very rapid (only one spawn is required), while it will be slower for coupled electronic states which are very different, e.g., a repulsive state intersecting a bound state. However, even in the latter case, we find that numerical convergence is usually reached with 3−5 spawns/event.

(H) The MIS Equation of Motion. The MIS (multiple independent spawning) approximation[22] serves to bring the formalism closer to the classical limit by neglecting such quantal interference effects that would, in any case, be washed out upon averaging over initial conditions. The technical approximation is to neglect the intrastate coupling in the FMS equation of motion (3.6) so that different nuclear basis functions on a given electronic state evolve independently of one another. The interstate coupling is kept the same. However, since much of the complexity of eq 3.6 is due to the intrastate terms, the MIS equation of motion

$$\mathrm{d}D_j^I/\mathrm{d}t = -i[(\mathbf{H}_{I,I} - i\dot{\mathbf{S}}_{I,I})_{j,j}D_j^I] - i\sum_{I'\neq I}\sum_k (\mathbf{H}_{I,I'})_{j,k}D_k^{I'} \quad (3.17)$$

is much simpler. The input to this equation is as defined earlier and the interstate multidimensional matrix elements are the same as in the FMS method. We do not use this approximation below, and it is recorded here for completeness. The primary computational advantage of the MIS is that it avoids the matrix inversion in (3.6). This is a consideration when the computational effort associated with the determination of potential energy surfaces and their couplings is not dominant. On the other hand, for first-principles nonadiabatic molecular dynamics, when the solution of the electronic problem is most time-consuming, there is no compelling computational advantage to MIS over FMS.

IV. Electronic Quenching in Na* + H_2

We have chosen the electronic quenching process of Na ($3p$ ^{2}P) by H_2 in order to demonstrate the multiple spawning method for polyatomic molecules. This is one of the most well-studied electronic quenching processes[14,87−97] and is important as a paradigm for electronic quenching. There is a conical intersection connecting the ground and first excited electronic states, corresponding to Na($3p$ ^{2}P) + H_2 and Na($3s$ ^{2}S) + H_2. The crossing of the two states is allowed in a C_{2v} symmetry (when the Na−H_2 Jacobi angle γ equals $\pi/2$) but is otherwise avoided. The ground-state potential energy surface is purely repulsive, while the first excited state is bound (with respect to excited-state Na atoms). Similar topologies of intersecting potential energy surfaces have been implicated in other internal conversion processes, for example, the Woodward−Hoffmann photochemically allowed ring openings.[98−101] In this work, we have examined the molecular scattering problem where Na* collides with H_2 with thermal energies. We focus on the quenching in this paper, but note that a related issue[87,93] is the "orbital following" which can be thought of as a nonadiabatic transition between the three excited states corresponding to the Na($3p$ ^{2}P) + H_2 exciplex, which are degenerate at infinite separation. This issue is explored in depth in a forthcoming paper, and here we wish to state only that the computations we describe did include all three excited states in addition to the ground state. We have used Cartesian coordinates to describe the dynamics, resulting in nine degrees of freedom for this problem. This means that we do not use any conserved quantities (e.g., the center of mass momentum) to reduce the dimensionality of the problem. The advantage is that the equations of motion are simpler and, in our experience this is an overwhelming consideration.

(A) Potential Energy Surfaces. The potential energy surfaces of Na−H_2 are best understood from the viewpoint of molecular orbital theory. We use the heuristic rule that the strength of bonding and antibonding interactions are in first order proportional to the square of the overlap between any two orbitals. Additionally, we will consider only the role of the three valence electrons. The H_2 molecule may be considered as having a doubly occupied σ orbital and an unoccupied σ^* orbital. Interaction with the s orbital of Na will be purely repulsive because the s orbital overlaps with the doubly occupied σ orbital of H_2, leading to a strong Pauli repulsion. Because the overlap of the Na s and H_2 σ^* orbitals is maximal for the collinear approach, one expects that this will lead to a maximal delocalization of the Na electron and partially mitigate the repulsion just cited. Similar arguments lead one to expect repulsive interactions between the H_2 molecule and Na*, with one exception—if the $3p$ orbital of Na is parallel to the H_2 molecular axis, there is no longer any overlap with the H_2 σ orbital and there is maximal delocalization of the Na electron. The interaction between the valence electrons is thus attractive, and a potential well could be expected. In fact, the above arguments are borne out by ab initio calculations.[88,94] Please note that the delocalization arguments should not be taken to imply that the Na*−H_2 exciplex is ionic in the usual sense of the word. The amount of charge transfer from Na* to H_2 is

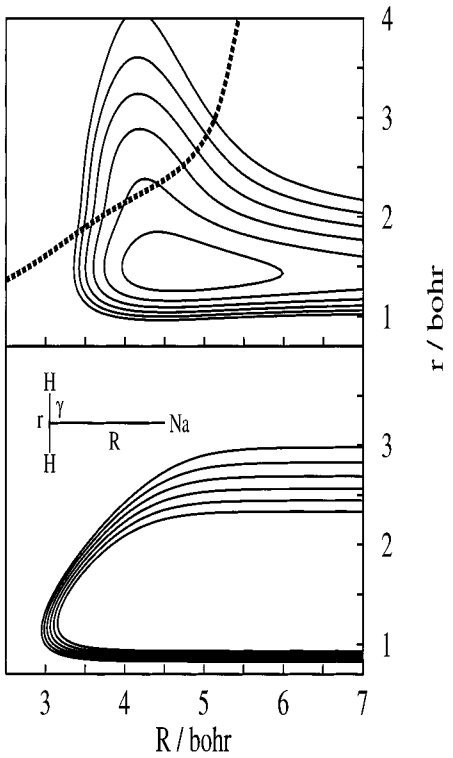

Figure 1. Two lowest diabatic potential energy surfaces, for a C_{2v} configuration, as a function of the Na to H_2 center of mass distance (R) and the H−H distance (r) in bohr; see inset. In both panels the contour lines are equally spaced between 1.75 and 3 eV. Lower panel: the repulsive ground state ($^2A_1$) potential where the Na valence electron is in the *3s* orbital. The zero of energy is taken with the Na atom and H_2 molecule at infinite separation, and the H−H distance at its equilibrium value. Upper panel: the lowest excited state ($^2B_2$) potential where the Na valence electron is in the *3p* orbital oriented parallel to the H_2 molecular axis. In C_{2v} symmetry the ground and lowest excited states cross, and the location of this crossing ("seam") is indicated by the dashed line. Because the electronic states are of different symmetry, they are uncoupled and this crossing persists in the adiabatic representation. The crossing seam is off the approach coordinate and accessing it requires a stretching of the H_2 bond. However, it is energetically accessible at the thermal collision energies used in the computations because at its lowest point ($r \sim 2.17$ bohr, $R \sim 4$ bohr) the seam lies somewhat below the electronic excitation energy (∼2.1 eV) of the Na atom.

very small; nevertheless, this delocalization will lower the kinetic energy of the Na* electron and stabilize the exciplex. We have used these arguments to develop an empirical functional form describing the potential energy surfaces needed, which was parametrized with reference to prior ab initio calculations.[88,94] The final result is also similar to other model surfaces which have been developed for this system, for example, the DIM model of Truhlar and co-workers.[102]

A semiquantitative realization of the above considerations builds on the angular overlap model.[103] The radial dependence of the intermolecular potentials is parametrized with Morse and exponentially repulsive functional forms, and the angular dependence is imparted by the overlap integrals between the relevant orbitals. We write the potential in the molecular frame, where the relevant variables are (see Figure 1) the Na−H_2 (center-of-mass) and H−H distances, and the Na−H_2 bending angle—R, r, and γ, respectively. The general potential is given as

$$V_{3s}(R,r,\gamma) = M_{H-H}(r) + S^2_{\sigma-s}X_{\sigma-s}(R) + \sum_{j=1,2} X_{Na-H_j}(|\mathbf{R}_{Na} - \mathbf{R}_{H_j}|) \quad (4.1)$$

TABLE 1: Parameters in Morse and Exponentially Repulsive Potentials and the Interstate Coupling (Eqs 4.1−4.6)[a]

	D_e	β	r_e
$M_{H-H}(r)$	0.1744	1.0276	1.40
$M'_{H-H}(R,r)$	0.1569 + 0.01744 tanh[1.49(R − 5)]	1.0276	1.40
$M_{Na-H_2}(R,r)$	0.05822 + 0.0424 tanh[1.429(r − 2.2)]	0.5500	3.92
	α	R_0	
$X_{\sigma-s}(R)$	2.9	3.4	
$X_{Na-H_i}(\lvert\vec{R}_{Na} - \vec{R}_{H_i}\rvert)$	4.0	2.5	
$X_{\sigma-Na(core)}(R)$	2.5	3.5	
$X_{\sigma-p}(R)$	0.3	3.0	
	Interstate Coupling		
$\lambda = 0.4$	$\alpha_r = 0.5$	$\alpha_R = 0.25$	

[a] Atomic units are used throughout.

$$V_{3p_i}(R,r,\gamma) = M'_{H-H}(r,R) + X_{\sigma-Na(core)}(R) + \sum_{j=1,2} X_{Na-H_j}(|\mathbf{R}_{Na} - \mathbf{R}_{H_j}|) + S^2_{\sigma^*-pi}M_{Na-H_2}(R) + S^2_{\sigma-pi}X_{\sigma-p}(R) + 2.1eV \qquad i = x, y, z \quad (4.2)$$

where the overlap integrals, $S^2_{\alpha-\beta} = |\langle a|b\rangle|^2$, refer to the angular factors only. The functions M and X represent Morse and exponentially repulsive functional forms, respectively:

$$M_i(r) = D^i_e(1 - \exp(-\beta^i(r - r^i_e)))^2 \quad (4.3)$$

$$X_i(R) = \exp(-\alpha^i(R - R^i_0)) \quad (4.4)$$

The well depths of the Morse potentials in the excited state, M'_{H-H} (r,R), are allowed to have a geometry dependence to account for the fact that the H−H bond should be slightly weakened by the delocalization of the Na *3p* electron. The parameters used in the Morse and exponentially repulsive forms are given in Table 1. For the purpose of evaluating the angular overlap, the σ and σ* orbitals of H_2 are treated as functions of *s* and *p* symmetry, i.e., we ignore the ellipsoidal shape of the orbitals. Defining the H−H bond as the z axis and the Na−H_2 plane as the x−z plane, the angular overlaps are given by

$$\langle\sigma|s\rangle = 1 \qquad \langle\sigma|p_x\rangle = \sin\gamma \qquad \langle\sigma|p_y\rangle = 0.6\sin\gamma \qquad \langle\sigma|p_z\rangle = 1 - \cos^2\gamma \quad (4.5)$$

where we have taken some liberties to improve the fit and overlaps not defined in eq 4.5 are identically zero.

Unfortunately, there is little quantitative information about the interstate coupling. Hence, we have simply used a functional form which is consistent with the symmetry-imposed requirement that the coupling vanish in C_{2v} and $C_{\infty v}$ nuclear configurations. We furthermore require that the coupling be continuous and that it vanishes at large Na−H_2 and H−H separations. The final form is

$$V_{s-p_i}(r,R,\gamma) = \lambda\sin(2\gamma)\exp(-\alpha_r r)\exp(-\alpha_R R) \qquad i = x, z \quad (4.6)$$

The parameters used are given in Table 1. Note that the Na($3p_y$)−H_2 state is rigorously uncoupled for all nuclear configurations by symmetry (see Figure 2). The Na($3p_x$)−H_2 and Na($3p_z$)−H_2 states are also coupled to one another, and for lack of other information we use the same form and parameters, except that λ is scaled by 0.3.

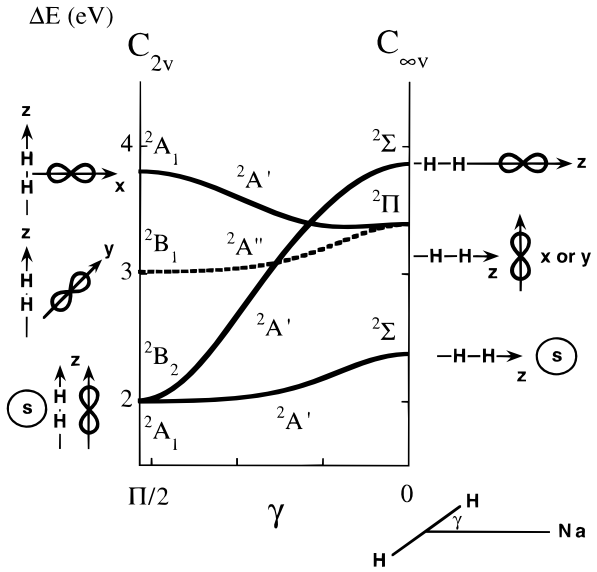

Figure 2. Bending (γ) angle dependence of the four diabatic potential energy surfaces for $R = 4$ bohr and $r = 2.17$ bohr. Energies are in eV, and the H_2 internuclear axis is defined as the z axis. Note that the labeling of the states varies with the bending angle, i.e., with the symmetry which is C_{2v} when $\gamma = \pi/2$ and $C_{\infty v}$ when $\gamma = 0$. To the right and left of the diagram we schematically represent the electronic states for Na + H_2 in C_{2v} and $C_{\infty v}$ symmetries. (The sphere labeled s represents a spherically symmetric *3s* orbital, whereas the ∞ symbol designates a *3p* orbital aligned along the *x*, *y*, or *z* axes. Note also that these potentials are defined in the molecular frame, so the axes are fixed in this frame and they rotate in the lab frame.) In C_{2v} symmetry the ground ($^2A_1$) and exited ($^2B_2$) state cross, whereas the other two *3p* states are degenerate in $C_{\infty v}$ symmetry. The symmetry labels imply that the $3p_y$ state (dashed line) is decoupled from the system whereas the ground *3s* state is coupled to both the $3p_z$ and $3p_x$ states which are also directly coupled to each other.

The resulting diabatic surfaces corresponding to the ground and lowest excited states, for nuclear geometries in C_{2v} symmetry are shown in Figure 1. The seam along which the two surfaces are degenerate is indicated by a dashed line. This degeneracy persists in the adiabatic representation because the two states belong to different irreducible representations in C_{2v} symmetry. Note the presence of a well in the excited state. In Figure 2, we show the angular variation of the diabatic potentials for H−H and Na−H_2 distances chosen to lie on the crossing seam. The state corresponding to Na($3p_y$)−H_2 is denoted with a dashed line to emphasize that it is uncoupled from the other three states. The Na($3p_z$)−H_2 and Na($3p_x$)−H_2 states cross at geometries which are of neither C_{2v} nor $C_{\infty v}$ symmetry. Hence, the adiabatic potentials corresponding to these states are not required to cross.

(B) Dynamics. The dynamics of Na* + H_2 were studied using the FMS method and the four potential energy surfaces described in the previous section. In all of the computations the collision is initiated with the Na* atom far from the H_2 molecule and at a relative (thermal) kinetic energy of 0.039 eV. The initial internal state of the H_2 molecule is a coherent vibrational state and a pendular rotational state, whereas the *3p* orbital is directed along a given axis in space that corresponds to excitation by linearly polarized laser at the Na D line. This orbital is then reexpressed in the molecule-fixed frame as a linear combination of the three space-fixed *3p* orbitals, and the initial wave function is propagated in time using the split operator procedure.[34,69] A nine-dimensional Cartesian coordinate system was used in the computations, and we monitored the amplitudes (magnitude and phase) of the four electronic states as well as other observables we deemed important for understanding the dynamics. As reported below, we have studied a wide range

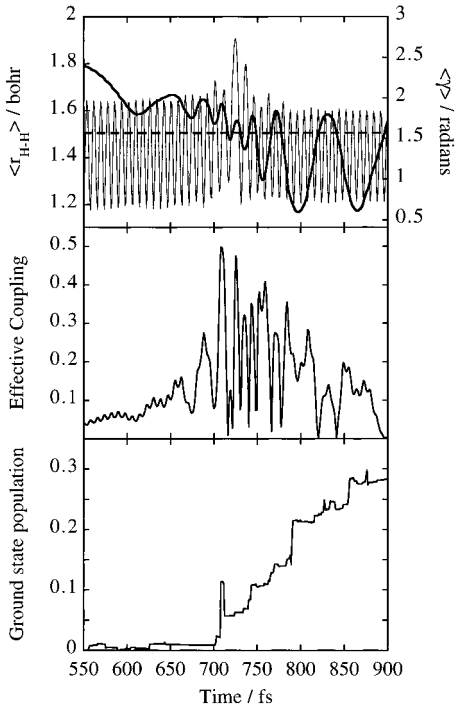

Figure 3. Typical collision at an impact parameter of 6 bohr and a relative kinetic energy of 0.039 eV. The initial internal state of the H_2 molecule is a coherent vibrational state and a pendular rotational state, and the zero of time is defined for the well-separated reactants. Lower panel: the ground-state population as a function of time in fs. Middle panel: the effective coupling between the ground and lowest excited state, defined (see eq 3.16) as the absolute value of the nonadiabatic coupling divided by the electronic energy gap, computed at the nuclear coordinates of the basis function representing the initial state. Upper panel: the expectation value of the H−H distance, r (thin line and left axis) and of the bending angle, γ, (heavy line and right axis) on the initially populated excited state. The dashed line indicates where $\gamma = \pi/2$ and the nonadiabatic coupling vanishes. Note the steplike increase in the ground-state population and the correlation between nonzero values of the effective coupling and changes in the ground-state population. As is evident from the middle and upper panels, the magnitude of the effective coupling is determined by both the bending angle and the H_2 internuclear distance, on longer and shorter time scales, respectively. Large effective coupling, and thus a large change in the population, requires a departure from C_{2v} symmetry, an extended H_2 bond length, and proximity of the three atoms (not shown). The fast modulation of the effective coupling at early times (and to a lesser extent at later times) is due to the molecular vibration.

of impact parameters and also examined the effect of rotational excitation of the H_2 molecule. The results presented below distinguish between single runs, i.e., a coherent initial state represented as a minimum uncertainty state, that enable us to study the mechanistic details of the dynamics, and results that are (incoherently) averaged over experimentally relevant initial conditions, such as the initial orientation. (This distinction is often invoked in quasi-classical computations.[104])

Unlike atom−atom collisions where the population transfer is often due to one or two nonadiabatic events, we find that in the Na* + H_2 system the quenching process is not direct and it involves many repeated transfers each of which is localized in time, as seen in the lower panel of Figure 3, where we plot the ground-state population as a function of time (in femtoseconds) for a single run (i.e., an initial coherent state) at an impact parameter of 6 bohr. In a typical run, the duration of the population transfer is very long (compared to the vibrational period of the H_2 molecule), and the collisions are rather "sticky". During this period the nonadiabatic coupling between the excited and the ground state is not monotonic in time but is switched on and off many times during the collision. As a measure of

the magnitude of the nonadiabatic coupling (which has been first discussed by Teller[8,9]), we plot in the middle panel of Figure 3 the absolute value of the nonadiabatic coupling divided by the electronic energy gap (eq 3.16), computed at the nuclear coordinates of the basis functions representing the initial state. The magnitude of the effective coupling is modulated by two motions which have very different time scales. The slow bending motion of the angle γ (upper panel and right axis of Figure 3) determines the magnitude of the interstate coupling (cf. eq 4.6), while the fast H_2 vibrational motion (upper panel and left axis of Figure 3) determines the electronic energy gap (cf. Figure 1). The sequential steplike increase in the ground population transfer is due to the repeated passage through a C_{2v} configuration (indicated by the dashed line in the upper panel of Figure 3), which is made possible by the sticky nature of the collision. Large effective coupling is clearly correlated with big changes in the ground-state population, and it requires a departure from C_{2v} symmetry as well as an extended H_2 bond length and proximity of the three atoms. The latter determines the duration of the collision which governs the overall period of population transfer.

Clearly the snarled quenching process shown in Figure 3 cannot be described as a single nonadiabatic event per collision and is thus very different from what is typically assumed in atom−atom collisions. The dynamics that we observe are of course due to the topography of the excited potential energy surface from which the quenching can occur directly. It has a shallow well along the atom−molecule approach coordinate (which is responsible for the sticky nature of the collisions) while the conical intersection is off this path and accessing it requires a large excursion in the H−H distance. Such a surface is reminiscent of many excited-state potential energy surfaces that have been proposed for other quenching processes,[10,98,105,106] and we therefore deem the random walk-like dynamics that we observe to be of general interest. It is also very interesting to note that in his 1937 paper,[8] Teller suggested that such multiple traversals of a conical intersection may be possible (and result in efficient quenching even if the transition probability per event is relatively small) "*if the potential surface is such that the molecular configuration will keep returning into the neighborhood of the apex of the cone*".

The multiple traversals of the conical intersection and the subsequent multiple nature of the population transfer result in a wave function that is delocalized on both the ground and the (initially populated) excited state. This delocalization evolves gradually during the quenching process as more basis functions are spawned on the ground electronic state and later also "back-spawned" from the ground state to the excited state. The buildup of delocalization in the wave functions is demonstrated in Figure 4, where we plot the reduced incoherent density as a function of the two distances R and r, at three points in time. (The zero of time is defined for the well-separated reactants, and the vertical scale is not the same in all panels because of the very different populations at different points in time and on different electronic states, so the population cannot be inferred from these plots.) The initial excited-state wave function (top left panel) is a coherent (i.e., minimum uncertainty) state with positive momentum along the atom molecule reaction coordinate. It is localized at a large $Na-H_2$ distance ($\sim$30 bohr) and around the H_2 equilibrium distance ($\sim$1.4 bohr). In the upper right panel we show the ground-state population at the middle of the collision when about half of the total quenching took place. At this point the ground state is already somewhat delocalized (in both coordinates), and because at this point in time the excited state wave function is still localized, we do not show it. At the end of the collision process, two lower panels in Figure 4, both the excited (bottom left panel) and the ground (bottom right panel) state components of the wave function are highly delocalized and are moving out toward larger $Na-H_2$ internuclear distances. Due to vibrational excitation (see below) on the ground electronic state, the ground-state component of the wave function is delocalized in both coordinates, yet the delocalization is of course more pronounced in the unbound R coordinate. (Recall that the ground-state $Na-H_2$ potential is purely repulsive.) Due to "back-spawning" the excited state (lower left panel) component of the wave function exits the collision in a bullet-like fashion, and the different components are localized at very different $Na-H_2$ internuclear distances: very small fractions of the excited-state wave function are still trapped in the excited-state shallow well, others are already at large R distances (between 25 and 50 bohr) and the main component of the excited-state wave function is at a distance of about 15 bohr. (Note that there is much less delocalization in the H−H distance on the excited electronic state because, unlike the ground-state component of the wave function, the excited-state component is not vibrationally excited.) This extended delocalization also implies that expectation values, of the position for example, cannot always be used to interpret the results as they do not necessarily represent the location of the wave function, because the dispersion can be high (as is seen, for $\langle R \rangle$ and to a lesser extent for $\langle r \rangle$, in Figure 4). Before proceeding to discuss averaged results (that correspond to an initial stationary state), we would like to stress that Figure 4 nicely demonstrates one of the most important and unique features of the spawning procedure (and more generally of our ansatz for the wave function, eq 3.1), namely the ability to describe very different dynamics on different electronic states and even within a given electronic state. Such qualitatively different dynamics (partially bound vs repulsive) on different electronic states cannot be described using mean field methods.

When studying the details of the dynamics, it is very instructive to analyze single runs. However, such (single) runs do not represent a typical initial state because a single run is not a stationary state of the Hamiltonian for the nonreacting species. A stationary state needs to be represented as a linear combination of several nuclear basis states. In the rest of this section we consider stationary states by averaging the results over the initial atom−molecule orientation (i.e., the polar and azimuthal angles). As expected, this averaging, inherent in representing a stationary state as a linear combination of basis states, washes out some of the dynamical details. (The steplike population transfer, for example, becomes smooth and continuous, yet it still extends over an extremely long time.) However, it does enable us to report such results as the quenching probability as a function of the initial impact parameter (Figure 5) which can be used to estimate the quenching cross section. According to Figure 5 quenching is still possible at a rather large impact parameter of about 10 bohr. This large value is not surprising if we consider the topography of the attractive excited electronic state and to the location of the seam. Although it is known that ionic states are not involved in this reaction (i.e., quenching does not proceed via a harpoon mechanism[107]), we do expect the quenching cross section to be relatively large. This is because the conical intersection is accessible at thermal energies and also because of the attractive nature of the excited-state potential. (Note, however, that the conical intersection is located on the repulsive branch of the excited-state potential.) A further consideration is that our computations predict that tunneling has a nonnegligible con-

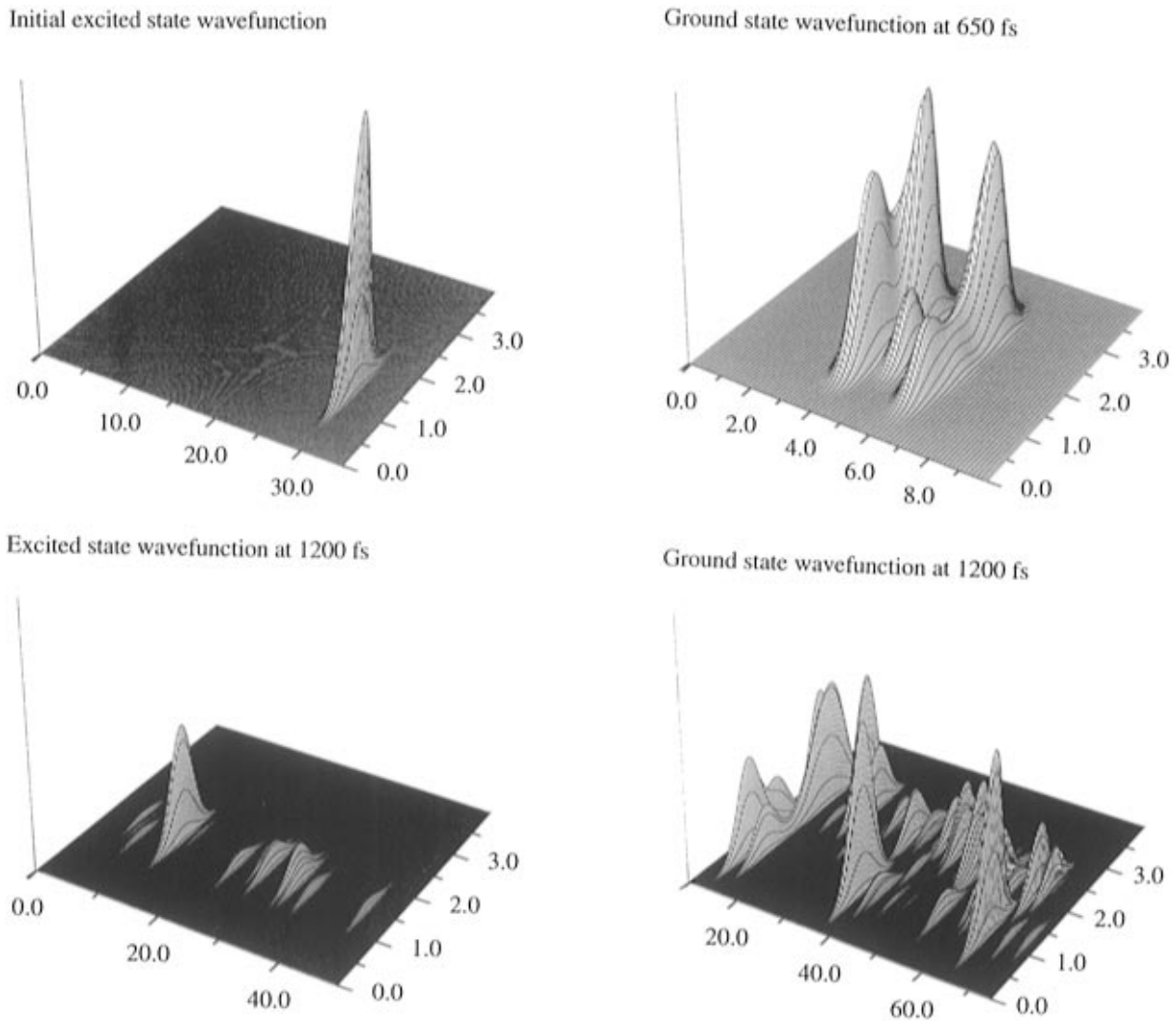

Figure 4. Four profiles of the probability density before, during and after the Na* + H_2 collision plotted vs the relative distance *R* and the H−H distance *r*. (The impact parameter in this collision is 4 bohr and note that the *R* scale in not the same in all panels.) The vertical (*z*) scale is not the same in all panels because whereas initially all the population is in the excited electronic state, after the collision 10% is left in the initial electronic state, 50% is in the ground electronic state, and 40% is in the other two *3p* states. (Hence, the population cannot be evaluated from these plots, which demonstrate only the spatial delocalization of the wave function.) Upper left panel: before the collision ($t = 0$) the initial wave function is localized at a large Na−H_2 distance and around r_{eq}. Upper right panel: the ground-state component of the wave function during the collision at a point in time ($t = 650$ fs) when about half of the total quenching already took place. Note that the ground state is already somewhat delocalized in *R* and that the H_2 molecule is formed vibrationally excited. At this time the excited-state wave function is still localized and therefore is not shown. Lower left panel: the excited-state component of the wave function after the quenching has essentially ceased ($t = 1200$ fs) and it is moving out. Note the wide range in *R* and the bullet-like fashion with which the excited-state component of the wave function exits. At the same point in time this spreading is even more pronounced for the ground-state component of the wave function (lower right panel).

tribution to the quenching probability. Since our potentials are qualitative and furthermore the magnitude of the nonadiabatic coupling is not known, we do not attempt to compare our results to the experimentally measured cross section but our computed estimate is of the order of about 20−25 Å^2, which is within the range of the experimentally measured one.[108] The more interesting question is of course the nonmonotonic dependence of the quenching probability on the initial impact parameter, and in particular its maximum. From careful inspection of individual runs, at each impact parameter, it seems that the only reasonable explanation for this maximum is that as the impact parameter is increased, the velocity (along the approach coordinate) in and about the nonadiabatic region decreases (on the average), because the relative kinetic energy is the same and the centrifugal barrier increases, and hence the quenching probability increases. Although the impact parameter may increase the quenching probability, by lowering the velocity in the nonadiabatic region, when it is large enough it blocks the access to the effective coupling region (due to the repulsive centrifugal term). Hence, there is a maximum in the quenching probability. Since the collision complex is long lived (on the time scale of the H_2 vibrational motion), and quenching occurs via many nonadiabatic events, this explanation is of course very qualitative and it cannot account for the magnitude of the maximum. Our results indicate that both the number of nonadiabatic events and the transfer probability per event are important in determining the final quenching probability in a collision.

Since many of the experiments on Na + H_2 were performed at elevated temperatures, we have also studied the effect of initial rotational excitation of the H_2 molecule on the quenching efficiency. In Figure 6 we compare the quenching probability (at an impact parameter of 1 bohr) for H_2 at $v = 0$, $j = 0$ and $v = 0$, $j = 3$. Although the duration of the population transfer is similar in both cases, the initial rotational excitation increases the quenching probability from 18% to 56%. We attribute this dramatic effect to efficient coupling between the rotation of the molecule and the bending motion that enables a more frequent

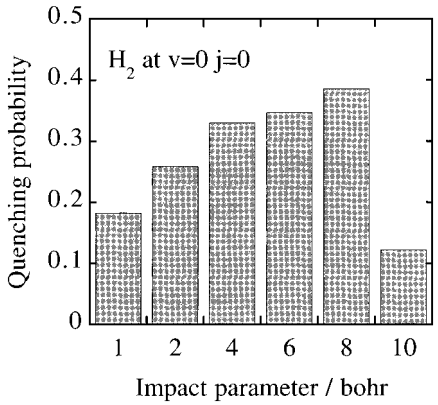

Figure 5. Quenching probability as a function of impact parameter (in bohr) for H_2 that is initially at $v = 0$, $j = 0$ and a relative kinetic energy of 0.039 eV. (At each impact parameter the results are averaged over 40 runs.) Although quenching does not proceed via a harpoon mechanism, there is a nonzero quenching probability at large impact parameters because of the excited-state potential well and because the seam is energetically accessible at thermal energies; see Figure 1. As discussed in the text, we attribute the maximum in the quenching probability to an interplay between two effects. As the impact parameter is increased, the velocity (along the approach coordinate) in and about the nonadiabatic region is decreased (on the average), because the relative kinetic energy is the same and the centrifugal barrier increases, and therefore the quenching probability increases, yet when the impact parameter is large enough it blocks the access to the effective coupling region (due to the repulsive centrifugal term) and hence the maximum in the quenching probability.

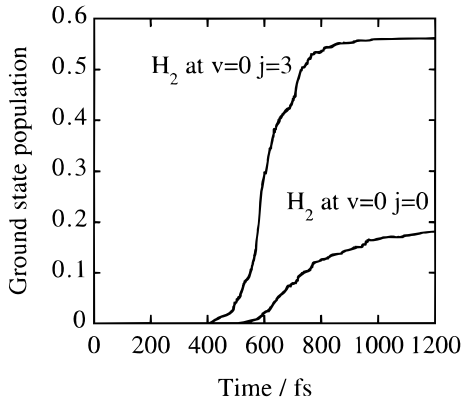

Figure 6. Ground-state probability as a function of time (in fs) for H_2 that is initially at $v = 0$, $j = 0$ and $v = 0$, $j = 3$, and an impact parameter of 1 bohr. As in Figure 5 the relative kinetic energy is 0.039 eV and the results are averaged over 40 runs. The quenching probability increases from about 18% to 56% due to the initial rotational excitation, and we ascribe this to efficient coupling between the rotation of the molecule and the bending of the exciplex that allows a more rapid and frequent sampling of the somewhat narrow nonadiabatic region about a C_{2v} symmetry.

and rapid sampling of the somewhat narrow nonadiabatic region about the configuration of C_{2v} symmetry. Naturally, we do expect that if the H_2 molecule is excited to higher rotational states ($j \sim 8$), the quenching probability will be lower than for rotationally cold H_2 molecules, both due to the filling of the attractive well by the repulsive centrifugal potential and due to the fast rotational motion of H_2, whose period scales as $1/j$.

Next we proceed to analyze the final states. As one can expect from the discussion of the effective coupling (which requires an extended H_2 bond length), the H_2 molecule on the ground electronic state is formed with much rotational and vibrational excitation. This is demonstrated by examining the $Na-H_2$ translational motion. In Figure 7 we plot the (incoherent) expectation value of the $Na-H_2$ distance as a function of

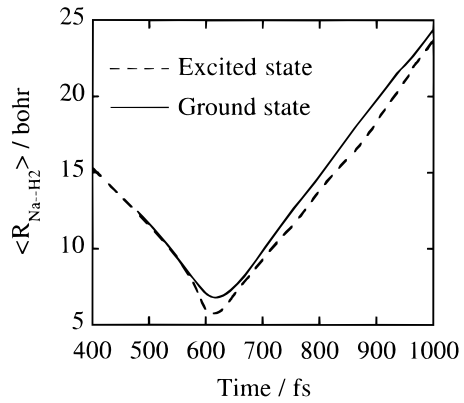

Figure 7. Expectation values of the $Na-H_2$ distance (in bohr) as a function of time (in fs) on the initially populated excited electronic state (dashed line) and the ground electronic state (full line). For clarity we show only a time slice of the collision. The averaged results are for an impact parameter of 1 bohr and all other parameters are as in Figure 5. The very similar slopes imply that as is to be expected from the topography of the potential energy surface and the position of the seam that is at an extended H_2 internuclear distance, effectively all the electronic energy (about 2.1 eV) is converted into internal excitation of the ground-state H_2 molecule. Note that initially the incipient ground electronic state overlaps the parent excited state.

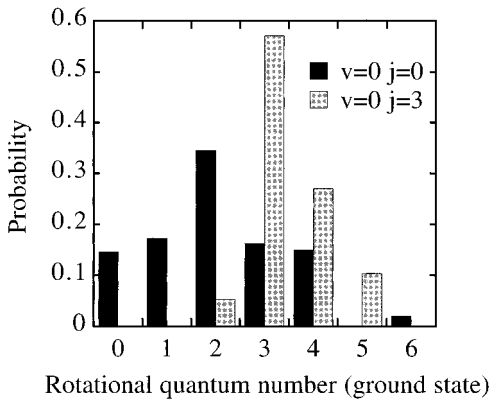

Figure 8. Final rotational distribution on the ground electronic state for H_2 that is initially at $j = 0$ (black bars) and at $j = 3$ (gray bars). All other parameters are as in Figure 6. For the initially rotationally cold H_2 molecules the final ground electronic state rotational distribution is hotter than that of the parent state (the most probable j is 2), whereas there is less excess rotational excitation on the ground electronic state (over and above that of the parent excited electronic state) when the initial j equals 3.

time (for clarity only a slice of the collision is shown) on both the ground (full line) and the excited (dashed line) electronic states. (The results are averaged over 40 runs at an impact parameter of 1 bohr.) The very similar slopes imply that effectively all the electronic energy (nearly 2.1 eV) is transferred into internal excitation of the H_2 molecule. (Note also that, as expected, and guaranteed by the spawning procedure, at early times the newly populated ground electronic state overlaps the parent excited state.) One can further analyze the internal excitation in terms of vibrational and rotational energies. We find that (for all impact parameters) the ground-state vibrational distribution peaks at $v = 4$, which is higher than the experimental value, $v = 3$. Even so, this agreement is quite good given the qualitative potential energy surface that we have used (and our further lack of knowledge concerning the details of the nonadiabatic coupling).

The final ground-state rotational distribution is shown in Figure 8 for H_2 that is initially at $j = 0$ (black bars) and at $j = 3$ (gray bars). This rotational distribution is calculated by using an incoherent sum over many single runs, in the spirit of

quasiclassical techniques. We reiterate here that each single run represents an approximate solution to the Schrödinger equation for a particular coherent initial state, and in principle we could sum the results coherently to recover the solution to the Schrödinger equation for a given stationary initial state. Computationally, it is easier to sum incoherently, but this implies that some information is lost irretrievably. One consequence of this is that rigorous selection rules need no longer be obeyed. For example, the angular dependence of the coupling (which the reader will recall was essentially dictated by symmetry and continuity requirements), implies a selection rule of $\Delta j = 0, \pm 2$ for $Na + H_2$. Yet this should not be expected from our results (and is not seen) because the final state we analyze is no longer a pure state. When these issues are important, or higher accuracy is desired, a coherent summation of the single runs be used should instead.

For the initially cold H_2 molecules we find that the ground-state distribution is hotter than the parent state (the most probable j is 2), whereas there is less excess rotational excitation (over and above the initial, parent, excited state) when the initial j is 3. This simply says that when j is greater than zero, a higher fraction of the electronic energy is dumped into vibration which is consistent with what we expect to happen when the collision time becomes somewhat shorter (due to the centrifugal potential). We also find, as expected, less rotational excitation in the ground state at an initial impact parameter of 10 bohr (not shown).

IV. Concluding Remarks

We have demonstrated that the proposed quantum mechanical approach is viable for a polyatomic system with nine degrees of freedom. The test case we used was not a simple one. The collision is "sticky" with many crossings of the region of effective coupling (Figure 3), several electronic states are coupled (Figure 2), quantum effects such as tunneling are important, and we worked in the laboratory system of coordinates which added three degrees of freedom to the problem. Yet we encountered no difficulties in connection with the multidimensional nature of the system. Partly this is because of the inherent feature of the method that much of the multidimensional character of the dynamics is carried out at the classical level. In particular, the size of the quantum mechanical basis set is not primarily determined by the number of degrees of freedom. Instead, the basis set is tailored to the problem using considerations of classical mechanics and knowledge (which is developed as the simulation progresses) of the nonadiabatic couplings. The computational efficiency of the method is demonstrated by the fact that we are able to compute a complete cross section for the quenching; see Figure 5.

The features of the $Na^* + H_2$ collision are perhaps special as compared to an atom−atom collision but are expected to be typical for polyatomic molecules. Low-energy collisions of polyatomic species are likely to be sticky so that the sporadic exit of the wave packet (Figure 4), is expected to be the norm. Note that this volleylike behavior is another manifestation of the quantum localization of the wave function. A fully delocalized state will have a finite, albeit small, amplitude everywhere. The important role of the bending motion of the exciplex (Figure 3 and further illustrated in Figure 6) may also be general.

The proposed method works well because the region of effective coupling is localized. There is no guarantee that this will always be true, but very often it is. The use of a nonstationary wave function means that describing the stationary internal states of the colliding partners (here, the vibration and rotation of H_2) requires using a linear combination of nuclear basis states to represent the initial state. On the other hand, because we use a nonstationary wave function, describing a pump−probe experiment, including the time dependence of the excitation and detection stages is relatively simple and applications to $Na^* + H_2$ will be the subject of a separate report.

Acknowledgment. We thank E. E. B. Campbell and K. L. Kompa for discussions. T.J.M. is grateful to the University of Illinois for generous start-up funds. R.D.L. acknowledges the support of the Air Force Office of Scientific Research and of the James Franck program. M.B.N. thanks the Rothschild Foundation for a Postdoctoral Fellowship and the United States-Israel Educational Foundation for a Fulbright Postdoctoral Award.

References and Notes

(1) Franck, J.; Jordan, P. *Anregung von Quantenspruengen durch Stoesse*; Julius Springer: Berlin, 1926.
(2) Mitchell, A. C. G.; Zemansky, W. M. *Resonance Radiation and Excited Atoms*; The McMillan Co.: New York, 1934.
(3) Wiley: E. J. B. *Collisions of the Second Kind*; Edward Arnold & Co.: London, 1937.
(4) Tully, J. C. Nonadiabatic Processes in Molecular Collisions. In *Dynamics of Molecular Collisions Part B*; Miller, W. H., Ed.; Plenum Press: New York, 1976.
(5) Child, M. S. Electronic Excitation: Nonadiabatic Transitions. In *Atom-Molecule Collision Theory*; Bernstein, R. B., Ed.; Plenum Press: New York, 1979.
(6) Nakamura, H. *Int. Rev. Phys. Chem.* **1991**, *10*, 123.
(7) Stueckelberg, E. C. G. *Helv. Phys. Acta* **1932**, *5*, 369.
(8) Teller, E. *J. Phys. Chem.* **1937**, *41*, 109.
(9) Teller, E. *Isr. J. Chem.* **1969**, *7*, 227.
(10) Koppel, H.; Domcke, W.; Cederbaum, L. S. *Adv. Chem. Phys.* **1984**, *57*, 59.
(11) Faist, M. B.; Levine, R. D. *J. Chem. Phys.* **1976**, *64*, 2593.
(12) Rebenstrost, F. In *Theoretical Chemistry, D.*; Henderson, D., Ed.; Academic Press: New York, 1979; Vol. VI.
(13) Baer, M. In *Thoery of Chemical Reaction Dynamics*; Baer, M., Ed.; CRC Press: Boca Raton, FL, 1984.
(14) Tawa, G. T.; Mielke, S. L.; Truhlar, D. G. *J. Chem. Phys.* **1994**, *100*, 5751.
(15) Kosloff, R. *Annu. Rev. Phys. Chem.* **1994**, *45*, 145.
(16) Manthe, U.; Koppel, H. *J. Chem. Phys.* **1990**, *93*, 1658.
(17) Muller, H.; Koppel, H.; Cederbaum, L. S. *J. Chem. Phys.* **1994**, *101*, 10263.
(18) Coker, D. F.; Xiao, L. *J. Chem. Phys.* **1995**, *102*, 496.
(19) Coalson, R. D. *J. Phys. Chem.* **1996**, *100*, 7896.
(20) Shin, S. *J. Phys. Chem.* **1996**, *100*, 7867.
(21) Martínez, T. J.; Ben-Nun, M.; Ashkenazi, G. *J. Chem. Phys.* **1996**, *104*, 2847.
(22) Martínez, T. J.; Ben-Nun, M.; Levine, R. D. *J. Phys. Chem.* **1996**, *100*, 7884.
(23) Pechukas, P. *Phys. Rev.* **1969**, *181*, 174.
(24) Tully, J. C. *J. Chem. Phys.* **1971**, *35*, 562.
(25) Neria, E.; Nitzan, A. *J. Chem. Phys.* **1993**, *99*, 1109.
(26) Webster, F.; Wang, E. T.; Rossky, P. J.; Friesner, R. A. *J. Phys. Chem.* **1994**, *98*, 4835.
(27) Billing, G. D. *Int. Rev. Phys. Chem.* **1994**, *13*, 309.
(28) Herman, M. F. *Annu. Rev. Phys. Chem.* **1994**, *45*, 83−111.
(29) Bittner, E. R.; Rossky, J. P. *J. Chem. Phys.* **1995**, *103*, 8130.
(30) Meyer, H.-D.; Miller, W. H. *J. Chem. Phys.* **1979**, *70*, 3214.
(31) Berendsen, H. J. C.; Mavri, J. *J. Phys. Chem.* **1993**, *97*, 13464.
(32) Tully, J. C. *J. Chem. Phys.* **1990**, *93*, 1061.
(33) Martínez, T. J.; Ben-Nun, M. *J. Chem. Phys.*, submitted.
(34) Martínez, T. J.; Levine, R. D. *Chem. Phys. Lett.* **1996**, *259*, 252.
(35) Ben-Nun, M.; Levine, R. D.; Jonas, D. M.; Fleming, G. R. *Chem. Phys. Lett.* **1996**, *245*, 629.
(36) Ben-Nun, M.; Levine, R. D.; Fleming, G. R. *J. Chem. Phys.* **1996**, *105*, 3035.
(37) Ford, W. K.; Wheeler, J. A. *Ann. Phys. N. Y.* **1959**, *7*, 287.
(38) Bernstein, R. B. *Adv. Chem. Phys.* **1966**, *10*, 75.
(39) Miller, W. H. *Adv. Chem. Phys.* **1974**, *25*, 69.
(40) Holland, P. R. *The Quantum Theory of Motion*; Cambridge University Press: Cambridge, 1993.
(41) Levine, R. D. *J. Chem. Phys.* **1972**, *56*, 1633.
(42) Schrödinger, E. *Naturwissenschaften* **1926**, *14*, 664.
(43) Glauber, R. J. *Phys. Rev.* **1963**, *131*, 2766.

(44) Caruthers, P.; Nieto, N. *Am. J. Phys.* **1965**, *33*, 537.
(45) Heller, E. J. *J. Chem. Phys.* **1975**, *62*, 1544.
(46) Coalson, R. D.; Karplus, M. *J. Chem. Phys.* **1982**, *90*, 301.
(47) Corbin, N.; Singer, K. *Mol. Phys.* **1982**, *46*, 671.
(48) Singer, K.; Smith, W. *Mol. Phys.* **1986**, *57*, 761.
(49) Skodje, R. T. *Chem. Phys. Lett.* **1984**, *109*, 227.
(50) Sawada, S.-I.; Heather, R.; Jackson, B.; Metiu, H. *J. Chem. Phys.* **1985**, *83*, 3009.
(51) Arickx, F.; Broeckhove, J.; Kesteloot, E.; Lathouwers, L.; Van Leuven, P. *Chem. Phys. Lett.* **1986**, *128*, 310.
(52) Lee, Y.-S. *Chem. Phys.* **1986**, *108*, 451.
(53) Huber, D.; Heller, E. J. *J. Chem. Phys.* **1987**, *87*, 5302.
(54) Huber, D.; Heller, E. J.; Littlejohn, R. G. *J. Chem. Phys.* **1988**, *89*, 2003.
(55) Huber, D.; Heller, E. J. *J. Chem. Phys.* **1988**, *89*, 4752.
(56) Huber, D.; Ling, S.; Imre, D. G.; Heller, E. J. *J. Chem. Phys.* **1989**, *90*, 7317.
(57) Grad, J.; Yan, Y. J.; Mukamel, S. *Chem. Phys. Lett.* **1987**, *134*, 291.
(58) Grad, J.; Yan, Y. J.; Haque, A.; Mukamel, S. *J. Chem. Phys.* **1987**, *86*, 3441.
(59) Dehareng, D. *Chem. Phys.* **1988**, *120*, 261.
(60) Kay, K. G. *J. Chem. Phys.* **1989**, *91*, 170.
(61) Ungar, L. W.; Cina, J. A. *J. Lumin.* **1994**, *58*, 89.
(62) Walton, A. R.; Manolopoulos, D. E. *Chem. Phys. Lett.* **1995**, *244*, 448.
(63) Wang, L.; Clary, D. C. *Chem. Phys. Lett.* **1996**, *262*, 284.
(64) Garaschuk, S.; Grossmann, F.; Tannor, D. *J. Chem. Soc., Faraday Trans.* **1997**, *93*, 781.
(65) Heller, E. J. *J. Chem. Phys.* **1976**, *64*, 63.
(66) Coalson, R. D. *J. Chem. Phys.* **1987**, *86*, 6823.
(67) Sawada, S.; Metiu, H. *J. Chem. Phys.* **1986**, *84*, 6293.
(68) Martínez, T. J.; Levine, R. D. *J. Chem. Phys.* **1996**, *105*, 6334.
(69) Martínez, T. J.; Levine, R. D. *J. Chem. Soc., Faraday Trans.* **1997**, *93*, 941.
(70) Martínez, T. J. *Chem. Phys. Lett.* **1997**, *272*, 139.
(71) Heller, E. J. *J. Chem. Phys.* **1981**, *75*, 2923.
(72) Davis, M. J.; Heller, E. J. *J. Chem. Phys.* **1984**, *80*, 5036.
(73) Ben-Nun, M.; Martínez, T. J.; Levine, R. D. *Chem. Phys. Lett.* **1997**, *270*, 319.
(74) Pulay, P. *Adv. Chem. Phys.* **1987**, *69*, 241.
(75) Helgaker, T.; Jorgensen, P. *Adv. Quantum Chem.* **1988**, *19*, 183.
(76) Lengsfield, B. H. I.; Yarkony, D. R. *Adv. Chem. Phys.* **1992**, *82*, 1.
(77) Smith, F. T. Elastic and Inelastic atom−atom scattering. In *Colorado Lectures in Theoretical Physics*; Benjamin: New York, 1968.
(78) Heller, E. J. *Acc. Chem. Res.* **1981**, *14*, 368.
(79) Zewail, A. H. *J. Phys. Chem.* **1996**, *100*, 12701.
(80) Fleming, G. R. *Chemical Applications of Ultrafast Spectroscopy*; Oxford University Press: New York, 1986.
(81) Press: W. H.; Teukolsky, S. A.; Vetterling, W. T.; Flannery, B. P. *Numerical Recipes in FORTRAN*; Cambridge Press: Cambridge, 1992.
(82) Ben-Nun, M.; Levine, R. D. *Chem. Phys.* **1995**, *201*, 163.
(83) Wigner, E. *Phys. Rev.* **1932**, *40*, 749.
(84) Moyal, J. E. *Proc. Cambridge Philos. Soc.* **1949**, *45*, 99.
(85) Davis, M. J.; Heller, E. J. *J. Chem. Phys.* **1979**, *71*, 3383.
(86) Kim, Y. S.; Noz, M. E. *Phase Space Picture of Quantum Mechanics*; World Scientific: Singapore, 1991.
(87) Hertel, I. V. *Adv. Chem. Phys.* **1981**, *45*, 341.
(88) Botschwina, P.; Meyer, W.; Hertel, I. V.; Reiland, W. *J. Chem. Phys.* **1981**, *75*, 5438.
(89) Reiland, W.; Tittes, U.; Hertel, I. V. **1982**.
(90) Truhlar, D. G.; Duff, J. W.; Blais, N. C.; Tully, J. C.; Garrett, B. C. *J. Chem. Phys.* **1982**, *77*, 764.
(91) Blais, N. C.; Truhlar, D. G. *J. Chem. Phys.* **1983**, *79*, 1334.
(92) Hering, P.; Cunha, S. L.; Kompa, K. L. *J. Phys. Chem.* **1987**, *91*, 5459.
(93) Campbell, E. E. B.; Schmidt, H.; Hertel, I. V. *Adv. Chem. Phys.* **1988**, *72*.
(94) Vivie-Riedle, R. d.; Hering, P.; Kompa, K. L. *Z. Phys. D* **1990**, *17*, 299.
(95) Pichler, G.; Motzkus, M.; Cunha, S. L.; Correia, R. R. B.; Kompa, K. L. *Nuovo Cimento* **1992**, *14*, 1065.
(96) Mielke, S. L.; Tawa, G. J.; Truhlar, D. G. *J. Am. Chem. Soc.* **1993**, *115*, 6436.
(97) Motzkus, M.; Pichler, G.; Kompa, K. L.; Hering, P. *Chem. Phys. Lett.* **1996**, *257*, 181.
(98) Celani, P.; Ottani, S.; Olivuccci, M.; Bernardi, F.; Robb, M. A. *J. Am. Chem. Soc.* **1994**, *116*, 10141.
(99) Olivucci, M.; Bernardi, F.; Celani, P.; Ragazos, I.; Robb, M. A. *J. Am. Chem. Soc.* **1994**, *116*, 1077.
(100) Bernardi, F.; Bottoni, A.; Olivucci, M.; Venturini, A.; Robb, M. *J. Chem. Soc., Faraday Trans.* **1994**, *90*, 1617.
(101) Lawless, M. K.; Wickham, S. D. *Acc. Chem. Res.* **1995**, *28*, 493.
(102) Halvick, P.; Truhlar, D. G. *J. Chem. Phys.* **1992**, *96*, 2895.
(103) Burdett, J. K. *Molecular Shapes: Theoretical Models of Inorganic Stereochemistry*; Wiley: New York, 1980.
(104) Truhlar, D. G.; Muckerman, J. T. Reactive Scattering Cross Sections: Quasiclassical and Semiclassical Methods. In *Atom-Molecule Collision Theory. A Guide for the Experimentalist*; Bernstein, R. B., Ed.; Plenum: New York, 1979.
(105) Reid, P. J.; Lawless, M. K.; Wickham, S. D.; Mathies, R. A. *J. Phys. Chem.* **1994**, *98*, 5597.
(106) Celani, P.; Bernardi, F.; Robb, M. A.; Olivucci, M. *J. Phys. Chem.* **1996**, *100*, 19364.
(107) Levine, R. D.; Bernstein, B. R. *Molecular Reaction Dynamics and Chemical Reactivity*; Oxford University Press: New York, 1987.
(108) Barker, J. H.; Weston, R. E. *J. Chem. Phys.* **1976**, *65*, 1427.